

Linear and nonlinear optical characteristics of Te nanoparticles-doped germanate glasses

Zhousu Xu^{1,3} · Qiangbing Guo¹ · Chang Liu¹ · Zhijun Ma⁴ · Xiaofeng Liu¹ · Jianrong Qiu²

Received: 26 July 2016 / Accepted: 19 September 2016 / Published online: 28 September 2016
© Springer-Verlag Berlin Heidelberg 2016

Abstract Te nanoparticles (NPs)-doped GeO_2 - MgO - B_2O_3 - Al_2O_3 - TeO_2 glasses were prepared by the conventional melt-quenching method. Based on X-ray photoelectron spectroscopy, Raman spectroscopy and transmission electron microscope observation, the coloration of the glass at high TeO_2 concentration is ascribed to the precipitation of elemental Te NPs with a size of 5–10 nm in the germanate glass. Optical absorption spectra and nonlinear optical (NLO) properties of the glass samples were analyzed by UV-3600 spectrophotometry and Z-scan technique, respectively. The nonlinear absorption coefficient (β) and the imaginary part of the third-order NLO susceptibility ($\text{Im}\chi^{(3)}$) were estimated to be 1.74 cm/GW and 1.142×10^{-12} esu for laser power of 95 μW , respectively. Due to the excellent NLO properties, the Te NPs-doped germanate glasses may have potential applications for ultrafast optical switch and photonics.

1 Introduction

Recently, metal nanoparticles (MNPs) and semiconductor nanoparticles (SNPs)-doped glasses have attracted much attention due to their unique linear and nonlinear optical (NLO) properties which are different from those of bulk metals [1–7]. They have a large third-order NLO susceptibility because of a large local-field enhancement factor and strong resonant absorption around the surface plasma peak of MNPs and large enhancement from the quantum confinement effect of SNPs [1, 2, 5]. The MNPs- and SNPs-doped glasses are usually fabricated by various processes such as melt-quenching, femtosecond laser irradiation and sol-gel methods [8–12]. Among these techniques, melt-quenching method remains the most convenient method as it offers facile access to a variety of glass systems doped with different crystalline phases with a simple and controllable process. By this process, noble metals such as Au and Ag as well as chalcogenide semiconductor quantum dots (QDs) can be precipitated in glasses of diverse chemical compositions, thus allowing for the investigation of optical properties and the quantum confinement effect [13, 14]. In comparison, the precipitation of non-noble MNPs and SNPs such as Si, Ga, Bi, Ge, Al and ZnTe has been reported only in a limited number of oxide glasses recently [5, 6, 15]. Lin et al. [5] reported that the metal and semiconductor NPs (Si, Cu, Ge, and Bi)-doped glasses prepared by the conventional melt-quenching method exhibit large third-order optical nonlinearities ($\chi^{(3)}$, about 10^{-8} esu) and ultrafast response time (within picoseconds). As they usually form strong covalent bond in the glass network, the precipitation of these NPs has been difficult and apparently quite selective for parent glass. However, their unique optical properties combined with the difficulty in the stabilization of their NPs in the colloidal solution phase have stimulated

✉ Xiaofeng Liu
xfliu@zju.edu.cn

✉ Jianrong Qiu
qjr@zju.edu.cn

¹ State Key Laboratory of Modern Optical Instrumentation, School of Materials Science and Engineering, Zhejiang University, Hangzhou 310027, China

² State Key Laboratory of Modern Optical Instrumentation, College of Optical Science and Engineering, Zhejiang University, Hangzhou 310027, China

³ Institute of Intelligent Optoelectronic Technology, Zhejiang University of Technology, Hangzhou 310014, China

⁴ State Key Laboratory of Luminescent Materials and Devices, and Institute of Optical Communication Materials, South China University of Technology, Guangzhou 510641, China

growing interest in the search of suitable glass systems for doping with these NPs, which have been expected to find applications in photonic fields, such as ultrafast all-optical switching, optical communication and optical storage.

In this investigation, we report the precipitate Te NPs in an oxide glass of $\text{GeO}_2\text{-MgO-B}_2\text{O}_3\text{-Al}_2\text{O}_3\text{-TeO}_2$ by the conventional melt-quenching method. The precipitation of Te NPs in the glasses was confirmed by X-ray photoelectron spectroscopy, Raman spectroscopy and transmission microscopy. The NLO properties of the Te NPs-doped glasses were investigated by using the Z-scan technique. The results reveal that the Te NPs-doped glasses exhibit excellent NLO properties, which are attractive for photonics applications.

2 Experimental

The germanate glass samples with the molar compositions of $(60 - x)\text{GeO}_2\text{-}x\text{TeO}_2\text{-}20\text{MgO-}15\text{B}_2\text{O}_3\text{-}5\text{Al}_2\text{O}_3$ (simplified as GT x , $x = 0, 0.5, 1$ and 3) were prepared by the conventional melt-quenching method. The raw materials are analytical grade MgO , H_3BO_3 , Al_2O_3 , 3 N TeO_2 and 5 N GeO_2 . For each batch of 20 g raw materials was mixed thoroughly and melted in alumina crucibles at 1500 °C for 30 min under air atmosphere. The melts were quenched on a stainless steel plate where the as-cast glasses were cooled down to room temperature. The glass samples were cut into small plates and then optically polished before optical characterizations.

The linear absorption spectra were recorded between 300 nm and 1800 nm using a UV-3600 spectrophotometer (Shimadzu Instruments). Raman spectra were recorded in the range of 100–1000 cm^{-1} using a LabRAM HR800 Raman spectrometer (Horiba Jobin Yvon Instruments) with 514 nm Ar^+ -ion laser as excitation source. The oxidation state of Te in glass was characterized using an ESCALAB 250XI photoelectron spectrometer (Thermo Instruments) with $\text{Al-K}\alpha$ X-ray as the excitation source, and the C 1s (284.8 eV) peak was used as the energy reference. The microstructure of the samples was observed by a Tecnai G2 F30 S-Twin transmission electron microscope (Philips-FEI Instruments), operating at 300 kV. The NLO properties of these glasses were measured by using Z-scan setup equipped with a Ti/sapphire laser with a wavelength of 800 nm, pulse width of 130 fs and repeating frequency of 1 kHz. The refractive index of the sample was measured by a Model 2010/M prism coupler (Metricon Instruments). All the measurements were taken at room temperature.

3 Results and discussion

The glass without TeO_2 is colorless and highly transparent in the visible and near infrared (NIR) region. With

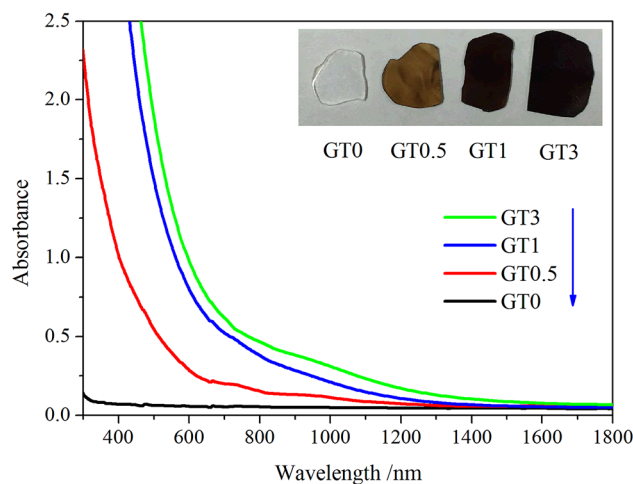


Fig. 1 Linear optical absorption spectra of the glasses. The inset is the photographs of the glasses

increasing in TeO_2 concentration, the as-cast glass changes its color from brown to black, as shown in the inset of Fig. 1. The linear optical absorption spectra of the glasses are also shown in Fig. 1. As shown clearly, with increasing in TeO_2 concentration, the optical absorption coefficient increases rapidly from 300 nm to 1200 nm. The change of optical absorption coefficient can be attributed to the presence of Te-related centers, presumable in the form of elemental Te.

To confirm the precipitation of elemental Te in the glasses, we recorded XPS and Raman spectra for the glasses. Figure 2a, b show the high-resolution XPS spectra in the Te $3d_{5/2}$ region for the glasses GT1 and GT3. The observed spectra can be divided into a band located at 573 eV and another band located at 576 eV, corresponding to the bonding energies of Te in the elemental Te and TeO_2 , respectively [16–18]. The Raman of the glasses GT0, GT0.5, GT1 and GT3 are shown in Fig. 2c. The spectrum shows two sharp bands located at around 120 and 140 cm^{-1} in the glasses GT1 and GT3, which are characteristic Raman signatures of elemental Te [19–21]. With increasing in TeO_2 concentration, the intensity of two characteristic bands increases, implying the growth of Te concentration. Due to the low TeO_2 concentration, the glass GT0.5 does not show two characteristic bands of elemental Te. From the above results of the XPS and Raman spectra analyses, we can conclude that part of TeO_2 is reduced to elemental Te by a decomposition reaction in the glass during high-temperature melting process.

To further confirm the precipitation of Te NPs in the glasses, the crushed glass powders of GT1 were observed with high-resolution transmission electron microscope (HRTEM). The HRTEM images reveal a large quantity of NPs in the glass GT1, as shown in Fig. 3. From a closer

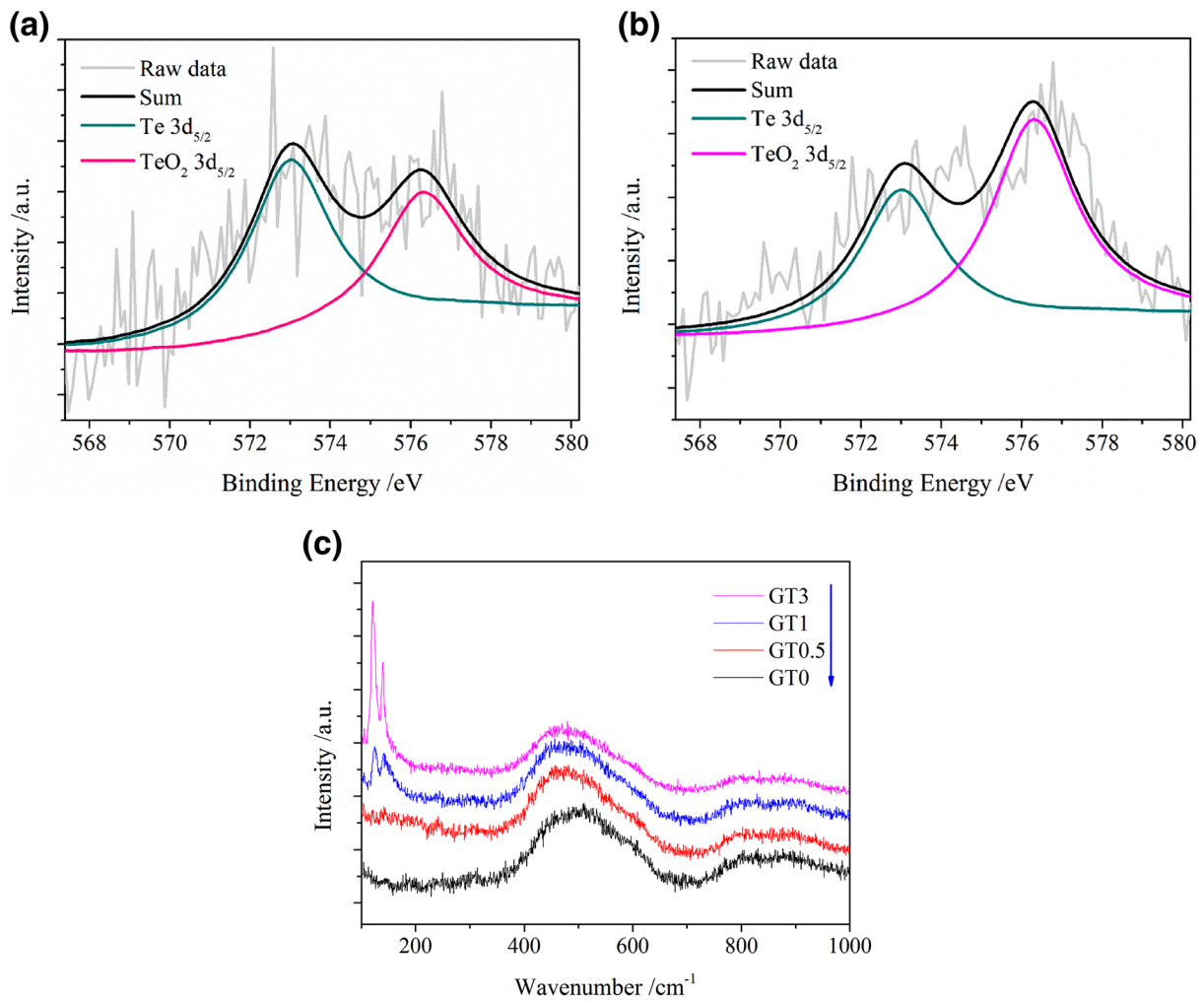


Fig. 2 High-resolution XPS spectra in the Te 3d_{5/2} region of the glasses: **a** GT1; **b** GT3. **c** Raman spectra of the glasses GT0, GT0.5, GT1 and GT3

observation of lattice fringes, the spacing of 0.235 and 0.314 nm is found, which correspond to the inter-planar distances of the (104) and (012) plane of Te (JCPDS No. 23-1000, $d_{104} = 0.231$ nm, $d_{012} = 0.311$ nm), respectively. In addition, the inter-planar spacing of 0.244, 0.274 and 0.300 nm match the (005) plane, (103) plane and (004) plane, which is absent from JCPDS No. 23-1000 as it is not observable by X-ray diffraction. All these results clearly indicate the presence of Te NPs in the glass.

We then examine the nonlinear optical response of the Te NPs-doped glasses by using the Z-scan technique. Typical normalized Z-scan transmittance curves for open-aperture measurement of glasses GT0 and GT1 are shown in Fig. 4. The results show that the germanate glass with 1 % TeO₂ exhibits clear NLO response at the excitation laser power of 95 μW, in sharp contrast to the germanate glass without TeO₂. The NLO response of the glasses changes dramatically with increasing of laser power.

According to NLO theory [22–25], the nonlinear absorption coefficient (β) can be determined by fitting the open-aperture Z-scan normalized transmittance curves using Eq. (1):

$$T(z) = 1 - \frac{\beta I_0 L_{\text{eff}}}{2\sqrt{2}[1 + (z/z_0)^2]} \tag{1}$$

where I_0 is the peak laser intensity at the focus, $z_0 = \frac{\pi \omega_0^2}{\lambda}$ is the diffraction length of the beam, ω_0 is the beam waist radius at the focus (~45 μm in our case) and $T(z)$ is the normalized transmission. L_{eff} is the effective thickness of the glass, determined by $L_{\text{eff}} = (1 - e^{-\alpha L})/\alpha$. L is the physical thickness of the glass measured to be 0.0809 cm, and α is the linear absorption coefficient estimated to be 10.816 cm⁻¹ at 800 nm. Consequently, L_{eff} of the glass is calculated to be 0.0539 cm. The calculated nonlinear absorption coefficient (β) at different laser power is revealed in Table 1, which shows that β is dependent on

Fig. 3 Typical HRTEM images of the glass GT1

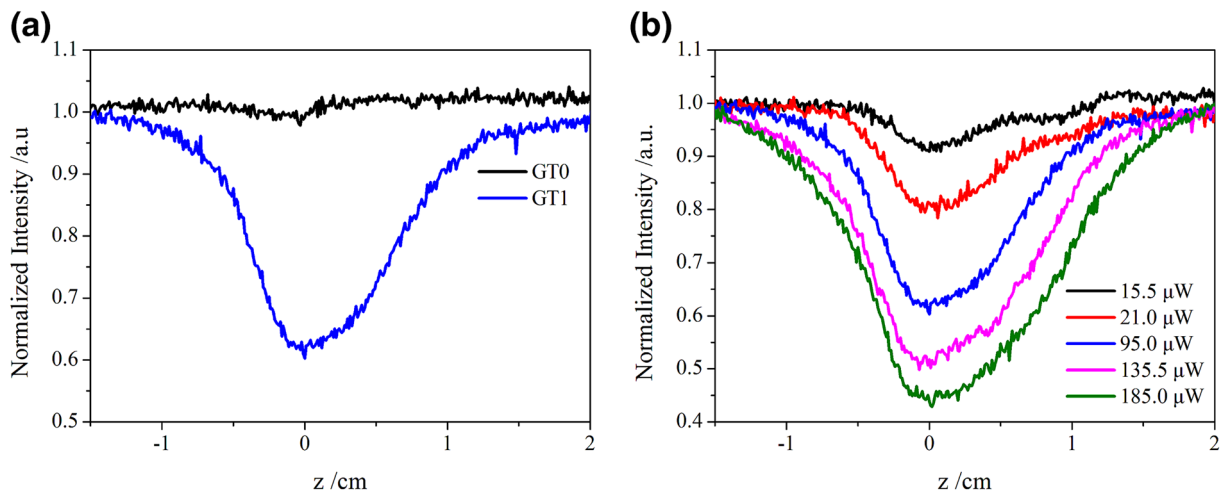
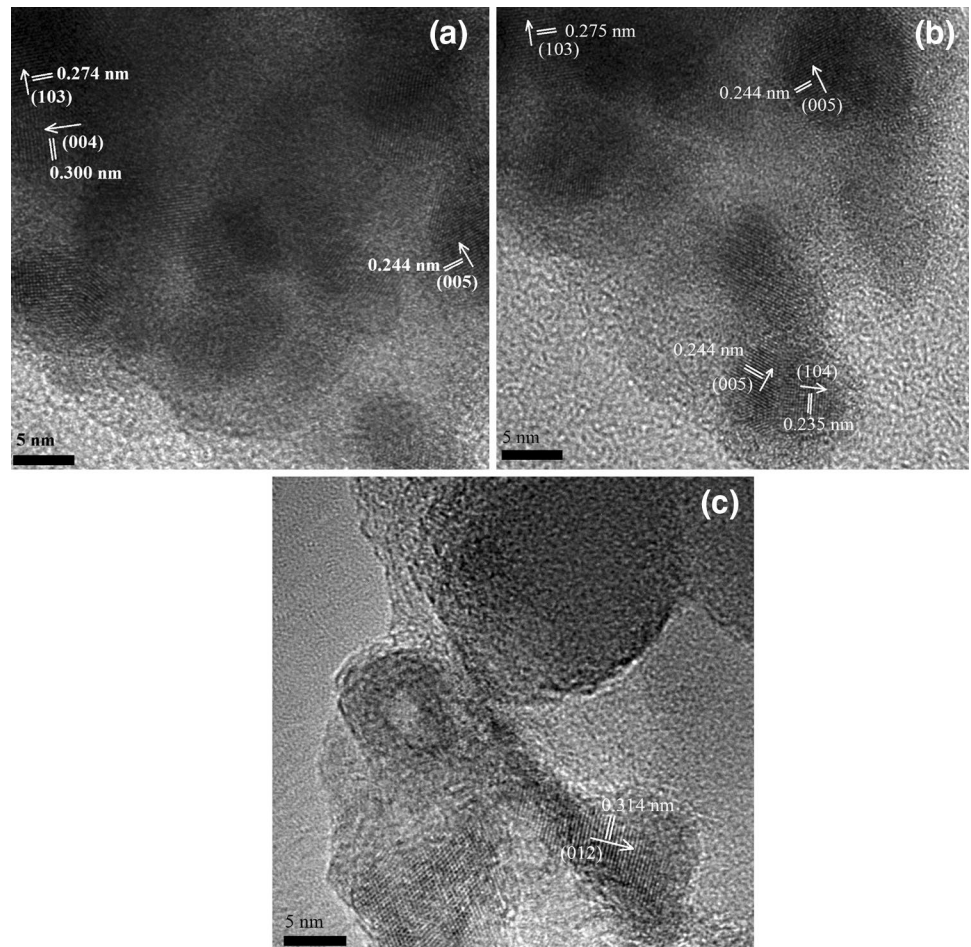


Fig. 4 Typical Z-scan normalized transmittance curves for open-aperture measurement of glass samples. **a** At laser power at 95 μW . **b** At different excitation powers for the glass sample GT1

the laser power. In particular, with laser power increased from 95 to 185 μW , the change of β becomes much slow. The imaginary part of the third-order NLO susceptibility ($\text{Im}\chi^{(3)}$) can be calculated by [24–26]

$$\text{Im}\chi^{(3)}(\text{esu}) = \frac{10^{-7} c \lambda n^2}{96\pi^2} \beta \tag{2}$$

where λ is the wavelength of the laser, c is the light speed in vacuum and $n = 1.61$ is the refractive index. Here, the

Table 1 β and $\text{Im}\chi^{(3)}$ at different laser powers

P (μW)	15.5	21	95	135.5	185
β (cm/GW)	2.53	4.13	1.74	1.57	1.34
$\text{Im}\chi^{(3)}$ (10^{-12} esu)	1.661	2.712	1.142	1.031	0.880

$\text{Im}\chi^{(3)}$ value is presented in Gaussian units (esu). The calculated $\text{Im}\chi^{(3)}$ at different laser power is also shown in Table 1. With laser power increased from 95 to 185 μW , the imaginary part of the third-order NLO susceptibility ($\text{Im}\chi^{(3)}$) is weakly dependent on the laser power.

The dependence of β and $\text{Im}\chi^{(3)}$ on laser power has also been reported for a SiO_2 glass, $\text{SiO}_2\text{-Na}_2\text{O-CaO}$ glass and $\text{SiO}_2\text{-Na}_2\text{O-B}_2\text{O}_3$ glass [27, 28]. The presence of a peak β value can be ascribed to the change of nonlinear absorption processes. There are many processes of nonlinear absorption, such as saturable absorption (SA) process and two-photon absorption (TPA) process. The TPA process is dominated at low laser power. With increasing of laser power, the TPA process becomes saturated and changes to SA process. This change leads to the β decreasing with increasing of laser power at high laser power [29, 30].

Tellurite glasses usually show large third-order NLO susceptibility up to 1.4×10^{-12} esu (TeO_2 glass) [31], $(1\text{--}2) \times 10^{-12}$ esu ($\text{TeO}_2\text{-ZnO-Li}_2\text{O-Bi}_2\text{O}_3$ glass) [32], and 2×10^{-12} esu ($\text{TeO}_2\text{-ZnO-Nb}_2\text{O}_5\text{-MoO}_3$ glass) [33], which is about 50 times larger than silica glass ($\sim 2.8 \times 10^{-14}$ esu) [31, 32] and 10 times larger than $\text{Bi}_2\text{O}_3\text{-GeO}_2\text{-TiO}_2$ glass ($\sim 1 \times 10^{-13}$ esu) [34]. Such a large third-order NLO susceptibility of tellurite glass may stem from the unique network structure. The tellurite glass consists of TeO_4 trigonal bipyramid unit, which has two equatorial and two axial oxygen atoms. The hybridization of Te atomic orbital in the axial plane is d^2p_z , while that in the equatorial plane is sp^2 . The empty $5d$ orbital and the $5s$ and $5p$ orbital of Te atom participate in the formation of the sp^3d hybrid molecular orbital of TeO_4 trigonal bipyramid. Previous report suggested that the large third-order NLO susceptibility of tellurite glass is ascribed to the empty $5d$ orbital of Te atom [31]. However, comparing to TeO_2 concentration (in mol%) in Ref. 31 (100 %), Ref. 32 (78 %), and Ref. 33 (70–78 %), TeO_2 concentration in this investigation is only 1 %. Therefore, the contribution of TeO_4 to the NLO properties is small, and large third-order NLO susceptibility in our investigation is mostly ascribed to Te NPs, not TeO_4 trigonal bipyramid. Our results indicated that the precipitation of Te nanoparticles leads to the observation of NLO property.

4 Conclusion

Glasses doped with Te NPs were prepared by the conventional melt-quenching method. The coloration and optical

properties of glasses have been investigated. The origin of coloration in the glasses is due to the precipitation of Te NPs, which was revealed by XPS spectra, Raman spectra and TEM observation. The NLO properties were obtained by Z-scan technique. The values of β and $\text{Im}\chi^{(3)}$ were estimated to be 1.34–4.13 cm/GW and $(0.880\text{--}2.712) \times 10^{-12}$ esu with laser power from 15.5 to 185 μW . The results show that the germanate glass doped with Te NPs exhibits excellent NLO properties, which may find potential applications in photonics and related fields.

Acknowledgments This work has been supported by the National Natural Science Foundation of China (Grant Nos. 51132004, 51472091, 11504323), the Natural Science Foundation of Zhejiang Province (Grant Nos. LY16F040005, LY15F050011, Q14E020009) and the Natural Science Foundation of Guangdong Province (Grant No. S2011030001349). This work was also supported by the Open Fund of the State Key Laboratory of High Field Laser Physics (Shanghai Institute of Optics and Fine Mechanics).

References

1. D.F. Eaton, Nonlinear optical materials. *Science* **253**(5017), 281–287 (1991)
2. W. Nie, Optical nonlinearity: phenomena, applications, and materials. *Adv. Mater.* **5**(7–8), 520–545 (1993)
3. H.B. Liao, R.F. Xiao, J.S. Fu, G.K.L. Wong, Large third-order nonlinear optical susceptibility of Au– Al_2O_3 composite films near the resonant frequency. *Appl. Phys. B Lasers Opt.* **65**(4–5), 673–676 (1997)
4. S. Qu, Y. Zhang, H. Li, J. Qiu, C. Zhu, Nanosecond nonlinear absorption in Au and Ag nanoparticles precipitated glasses induced by a femtosecond laser. *Opt. Mater.* **28**(3), 259–265 (2006)
5. G. Lin, F. Luo, H. Pan, M.M. Smedskjaer, Y. Teng, D. Chen, J. Qiu, Q. Zhao, Universal preparation of novel metal and semiconductor nanoparticle glass composites with excellent nonlinear optical properties. *J. Phys. Chem. C* **115**(50), 24598–24604 (2011)
6. G. Lin, D. Tan, F. Luo, D. Chen, Q. Zhao, J. Qiu, Linear and nonlinear optical properties of glasses doped with Bi nanoparticles. *J. Non-Cryst. Solids* **357**(11–13), 2312–2315 (2011)
7. S. Zhou, Q. Guo, H. Inoue, Q. Ye, A. Masuno, B. Zheng, Y. Yu, J.R. Qiu, Topological engineering of glass for modulating chemical state of dopants. *Adv. Mater.* **26**(47), 7966–7972 (2014)
8. Y. Hamanaka, A. Nakamura, S. Omi, N. Del Fatti, F. Vallee, C. Flytzanis, Ultrafast response of nonlinear refractive index of silver nanocrystals embedded in glass. *Appl. Phys. Lett.* **75**(12), 1712–1714 (1999)
9. D. Tan, Y. Yamada, S. Zhou, Y. Shimotsuma, K. Miura, J. Qiu, Carbon nanodots with strong nonlinear optical response. *Carbon* **69**, 638–640 (2014)
10. J. Qiu, M. Shirai, T. Nakaya, J. Si, X. Jiang, C. Zhu, K. Hirao, Space-selective precipitation of metal nanoparticles inside glasses. *Appl. Phys. Lett.* **81**(16), 3040–3042 (2002)
11. S. Selvan, T. Hayakawa, M. Nogami, Y. Kobayashi, L. Marzán, Y. Hamanaka, A. Nakamura, Sol–gel derived gold nanoclusters in silica glass possessing large optical nonlinearities. *J. Phys. Chem. B* **106**(39), 10157–10162 (2002)
12. H. Zhang, Z. Hu, Z. Ma, M. Gecevicius, G. Dong, S. Zhou, J. Qiu, Anisotropically enhanced nonlinear optical properties of ensembles of gold nanorods electrospun in polymer nanofiber film. *ACS Appl. Mater. Interfaces* **8**(3), 2048–2053 (2016)

13. X.N. Liu, D.Z. Yao, H.M. Zhou, F. Chen, G.G. Xiong, Third-order nonlinear optical response in quantum dot-metal nanoparticle hybrid structures. *Appl. Phys. B Lasers Opt.* **113**(4), 603–610 (2013)
14. E.V. García-Ramírez, S. Almaguer-Valenzuela, O. Sánchez-Dena, O. Baldovino-Pantaleón, J.A. Reyes-Esqueda, Third-order nonlinear optical properties of colloidal Au nanorods systems: saturable and reverse-saturable absorption. *Opt. Express* **24**(2), A154–A167 (2016)
15. X. Du, L. Zhang, G. Dong, K. Sharafudeen, J. Wen, D. Chen, Q. Qian, J. Qiu, Coloration and nonlinear optical properties of ZnTe quantum dots in ZnO–TeO₂–P₂O₅ Glasses. *J. Am. Ceram. Soc.* **97**(1), 185–188 (2014)
16. YuA Teterin, V.I. Nefedov, M.F. Churbanov, AYu. Teterin, K.I. Maslakov, E.V. Zorin, X-ray photoelectron study of Te–W–O and Te–W–La–O glasses. *Inorg. Mater.* **43**(8), 888–896 (2007)
17. Z.A. Jin, A.D. Zhang, A. Kovalskiy, I. Biaggio, A near-IR transmitting black glass synthesized from 70 % TeO₂–25 % ZnO–5 % ZnS. Presented at the 2009 Conference on Lasers and Electro-Optics & Quantum Electronics and Laser Science Conference, Baltimore, Maryland, May 31–June 5, 2009 (Paper no. JWA25)
18. H. Hayashi, N. Shigemoto, S. Sugiyama, N. Masaoka, K. Saitoh, X-ray photoelectron spectra for the oxidation state of TeO₂–MoO₃ catalyst in the vapor-phase selective oxidation of ethyl lactate to pyruvate. *Catal. Lett.* **19**(2–3), 273–277 (1993)
19. J. Sun, Q. Nie, X. Wang, S. Dai, X. Zhang, B. Bureau, C. Bousard, C. Conseil, H. Ma, Structural investigation of Te-based chalcogenide glasses using Raman spectroscopy. *Infrared Phys. Technol.* **55**(4), 316–319 (2012)
20. G.D. Keskar, R. Podila, L.H. Zhang, A.M. Rao, L.D. Pfefferle, Synthesis and Raman spectroscopy of multiphasic nanostructured Bi–Te networks with tailored composition. *J. Phys. Chem. C* **117**(18), 9446–9455 (2013)
21. Z. Xu, C. Xu, Q. Guo, X. Liu, J. Qiu, Effect of TeO₂ on near-infrared emission from bismuth centers in borogermanate glasses. *J. Am. Ceram. Soc.* **99**(3), 760–764 (2016)
22. X. He, H. Zhang, R. Wei, Z. Ma, J. Qiu, M. Zhang, Q. Zeng, A. Liu, R. He, Nonlinear saturable absorption of nanoscaled Bi₂Te₃/PMMA composite film. *Phys. E* **81**, 71–76 (2016)
23. R. Naderali, A. Jafari, H. Motiei, Nonlinear optical properties of carboxymethyl starch nanocomposite by Z-scan technique using a Nd-YAG laser. *Appl. Phys. B Lasers Opt.* **120**(4), 681–687 (2015)
24. D. Potamianos, I. Papadakis, E. Kakkava, A.B. Bourlinos, G. Trivizas, R. Zboril, S. Couris, Nonlinear optical response of gold-decorated nanodiamond hybrids. *J. Phys. Chem. C* **119**(43), 24614–24620 (2015)
25. S. Mansoor, A.A. Said, T. Wei, D.J. Hagan, E.W. Stryland, Sensitive measurement of optical nonlinearities using a single beam. *IEEE J. Quantum Electron.* **26**(4), 760–769 (1990)
26. N. Liaros, P. Aloukos, A. Kolokithas Ntoukas, A. Bakandritsos, T. Szabo, R. Zboril, S. Couris, Nonlinear optical properties and broadband optical power limiting action of graphene oxide colloids. *J. Phys. Chem. C* **117**(13), 6842–6850 (2013)
27. R.A. Ganeev, A.I. Rysanyansky, A.L. Stepanov, T. Usmanov, Saturated absorption and nonlinear refraction of silicate glasses doped with silver nanoparticles at 532 nm. *Opt. Quantum Electron.* **36**(10), 949–960 (2004)
28. X. Yang, W. Xiang, H. Zhao, H. Liu, X. Zhang, X. Liang, Nonlinear saturable absorption of the sodium borosilicate glass containing Bi₂S₃ nanocrystals using Z-scan technique. *J. Alloys Compd.* **509**(26), 7283–7289 (2011)
29. K. Wang, H. Long, M. Fu, G. Yang, P.X. Lu, Intensity-dependent reversal of nonlinearity sign in a gold nanoparticle array. *Opt. Lett.* **35**(10), 1560–1562 (2010)
30. B.H. Yu, D.L. Zhang, Y.B. Li, Q.B. Tang, Nonlinear optical behaviors in a silver nanoparticle array at different wavelengths. *Chin. Phys. B* **22**(1), 014212 (2013)
31. S. Kim, T. Yoko, S. Sakka, Linear and nonlinear optical properties of TeO₂ glass. *J. Am. Ceram. Soc.* **76**(10), 2486–2490 (1993)
32. G. Murugan, T. Suzuki, Y. Ohishi, Raman characteristics and nonlinear optical properties of tellurite and phosphotellurite glasses containing heavy metal oxides with ultrabroad Raman bands. *J. Appl. Phys.* **100**(2), 023107 (2006)
33. R. Jose, Y. Ohishi, Higher nonlinear indices, Raman gain coefficients, and bandwidths in the TeO₂–ZnO–Nb₂O₅–MoO₃ quaternary glass system. *Appl. Phys. Lett.* **90**(21), 211104 (2007)
34. F. Chen, B. Song, C. Lin, S. Dai, J. Cheng, J. Heo, Glass formation and third-order optical nonlinear characteristics of bismuth-antem glasses within Bi₂O₃–GeO₂–TiO₂ pseudo-ternary system. *Mater. Chem. Phys.* **135**(1), 73–79 (2012)